RSC Advances

PAPER

View Article Online
View Journal | View Issue

Cite this: *RSC Adv.*, 2023, **13**, 8890

Synthesis of tetrazoles catalyzed by a new and recoverable nanocatalyst of cobalt on modified boehmite NPs with 1,3-bis(pyridin-3-ylmethyl) thiourea†

Arida Jabbari, *[a] Parisa Moradi [b] and Bahman Tahmasbi [b]

Received 25th November 2022
Accepted 1st March 2023

DOI: 10.1039/d2ra07510e

rsc.li/rsc-advances

In the first part of this work, boehmite nanoparticles (BNPs) were synthesized from aqueous solutions of NaOH and $Al(NO_3)_3 \cdot 9H_2O$. Then, the BNPs surface was modified using 3-choloropropyltrimtoxysilane (CPTMS) and then 1,3-bis(pyridin-3-ylmethyl)thiourea ($(PYT)_2$) was anchored on the surface of the modified BNPs (CPTMS@BNPs). In the final step, a complex of cobalt was stabilized on its surface (Co-$(PYT)_2$@BNPs). The final obtained nanoparticles were characterized by FT-IR spectra, TGA analysis, SEM imaging, WDX analysis, EDS analysis, and XRD patterns. In the second part, Co-$(PYT)_2$@BNPs were used as a highly efficient, retrievable, stable, and organic–inorganic hybrid nanocatalyst for the formation of organic heterocyclic compounds such as tetrazole derivatives. Co-$(PYT)_2$@BNPs as a novel nanocatalyst are stable and have a heterogeneous nature; therefore, they can be recovered and reused again for several consecutive runs without any re-activation.

1 Introduction

In recent years, boehmite nanoparticles (BNPs) have attracted interest from both practical and fundamental viewpoints.[1,2] In fact, boehmite is aluminum oxyhydroxide (γ-AlOOH) and it is the most stable phase of alumina after gibbsite.[3–6] Boehmite consists of double sheets of oxygen octahedron with Al-atoms at their centers.[7–10] The boehmite sheets themselves are composed of octahedral chains with a cubic orthorhombic unit cell.[2,11] Also, BNPs are very stable and they are not moisture or air sensitive.[12,13] Therefore, BNPs can synthesized in aqueous media without inert atmosphere by available materials such as inexpensive aluminum salts.[14] The physical and chemical properties of boehmite are strongly dependent on the experimental condition of its synthesis.[13] For example, BNPs were synthesized by different methods such as hydrolysis of aluminum salts,[2] precipitation in an aqueous solution from aluminum salt solutions,[15] hydrothermal procedures,[2] solid state decomposition of gibbsite,[16] sol–gel procedures,[17] and solvothermal procedures.[2] Boehmite contains high aggregation of hydroxyl groups on its surface, that supply suable places for modify of its surface with other functional groups such as electrophilic or nucleophilic sites which are enable to immobilization of suitable ligands or metal complexes.[18–22] Therefore BNPs can be used as an excellent support for fabrication of wide range of heterogeneous catalysts.[2] BNPs were utilized as support for stabilization of acidic,[23] basic,[24] metallic catalysts[25,26] and organo- or ionic[22] supported catalysts. More addition, boehmite nanoparticle have several unique attributes such as good surface area, easy availability, non-toxicity, chemical resistance, mechanical strength, thermal stability, good conductivity, high hardness, low cost, excellent biocompatibility, high abrasive and corrosion resistance.[1,2,22] However, BNPs are also have some disadvantages, such as impurities content (*e.g.* nitrate ions) that led to lower their crystallinity. This impurities concentration may affect properties of the surface property and pore structure of boehmite. In the other hand, BNPs may converts into a γ-Al_2O_3 in the high temperatures, but this cannot effect on the catalysis application of BNPs in organic reactions. Because organic reactions take place at temperatures lower than the BNPs phase change. Therefore, Boehmite nanomaterials have also attracted attention in absorbent,[27] coatings,[28] flame retardant,[29] optical material,[30] ceramics,[31] vaccine adjuvants,[32] cosmetic products,[2,33] pillared clays and sweep-flocculation for fresh water treatment.[13] Consequently, we investigated a new complex of cobalt with 1,3-bis(pyridin-3-ylmethyl)thiourea on boehmite nanoparticle (Co-$(PYT)_2$@BNPs) as a reusable nanocatalyst in the synthesis of tetrazole derivatives. Because tetrazole compounds are an important group of medicinal and organic compounds which possess many uses in several fields such as coordination chemistry, synthetic organic chemistry, drugs, medicinal

[a]*Department of Chemistry, Qeshm Branch, Islamic Azad University, Qeshm, Iran. E-mail: arida_jabbari@yahoo.com*

[b]*Department of Chemistry, Faculty of Science, Ilam University, P.O. Box 69315516, Ilam, Iran*

† Electronic supplementary information (ESI) available. See DOI: https://doi.org/10.1039/d2ra07510e

chemistry as surrogates for carboxylic acids, the photographic industry, catalysis technology, and organometallic chemistry as effective stabilizers of metallopeptide structures.[34–41]

2 Experimental

2.1 Materials and instruments

Solvents and chemical materials in this project bought from Iranian companies, Aldrich, Merck or Fluka and used sans any purification.

The particle morphology and particle diameters of synthesized catalyst studied *via* FESEM-TESCAN MIRA III Scanning-Electron-Microscope (SEM) from Czechia. In addition, FESEM-TESCAN MIRA III used for type, content and number of elements (*via* WDX and SEM-EDS analysis) of the nanocatalyst. XRD diffraction of the nanocatalyst recorded by a PW1730 device madding Philips Company of Netherlands. IR spectra recorded using KBr pills in a VRTEX 70 model Bruker IR spectrometer. TGA diagram of the nanocatalyst recorded by a SDT Q600 V20.9 Build 20 Thermal Analysis device under air atmosphere in the temperature range of 30–800 °C. NMR spectra of the tetrazoles registered *via* Bruker-DRX-400 spectrometer.

2.2 Synthesis of 1,3-bis(pyridin-3-ylmethyl)thiourea ($(PYT)_2$) ligand (3)

In a round-bottomed flask, 3-(aminomethyl)pyridine (1, 10 mmol) added to CS_2 (5 mmol) in H_2O and stirred at room temperature for 7 h (Scheme 1). The reaction progress consecutively checked by TLC (EtOAc: *n*-hexane, 1 : 2). Since this reaction is exothermic, the temperature increases during the reaction and so this temperature is sufficient for release H_2S (confirmed by smell and blackening of lead acetate paper). After performance of the reaction, the water-insoluble product filtered, and then recrystallized from hot water and ethanol (1 : 1 v/v).

The structure of $(PYT)_2$ ligand was characterized by ^1H NMR and FT-IR spectroscopies:

2.2.1 1,3-bis(pyridin-3-ylmethyl)thiourea ($(PYT)_2$). ^1H NMR (400 MHz, DMSO-d_6): $\delta_H = 5.50$ (s, 2H), 8.46–8.44 (d, $J = 8$ Hz, 2H), 8.22 (br, 2H), 7.69–7.66 (d, $J = 12$ Hz, 2H), 7.37–7.33 (d of d, $J = 8$ Hz, $J = 4$ Hz, 2H), 4.69 (s, 4H) ppm.

IR (KBr) cm^{-1}: 3272, 3184, 3000, 2923, 2853, 2359, 1913, 1529, 1473, 1422, 1298, 1237, 1193, 1101, 1027, 973, 918, 805, 770, 708, 616, 535.

2.3 Synthesis of the catalyst

50 mL of aqueous solution of sodium hydroxide (6.490 g) was added to 30 mL of aqueous solution of aluminum nitrate (20 g) as drop to drop under vigorous stirring. The resulting milky mixture was transferred in the ultrasonic bath (for 3 h at room temperature). The resulted BNPs was filtered and washed by distilled water. The obtained BNPs were kept in the oven at 220 °C for 4 h. Then, BNPs were modified by (3-chloropropyl)triethoxysilane (CPTMS) to preparation of CPTMS@BNPs. The CPTMS@BNPs formed matching to reported method in literature.[41,42] As reported, the BNPs (1.5 g) dispersed in normal hexane, and then CPTMS (2 mL) injected and the mixture stirred for 24 h under reflux conditions that the modified BNPs by CPTMS (CPTMS@BNPs) were produced. The prepared CPTMS@BNPs were filtered, washed by ethanol (EtOH) and dried at room temperature. In order to immobilization of $(PYT)_2$ ligand (3) on CPTMS@BNPs, 1 g of CPTMS@BNPs refluxed with $(PYT)_2$ in toluene for 40 h. After then, obtained $(PYT)_2$@BNPs isolated *via* filtration, washed by DMSO and EtOH, afterward dried at 60 °C. Finally, $(PYT)_2$@BNPs (1 g) was dispersed in EtOH, and then $Co(NO_3)_2 \cdot 6H_2O$ injected to the obtained mixture and then stirred for 24 h under reflux conditions. The resulting catalyst (Co-$(PYT)_2$@BNPs) filtered, washed and dried at 60 °C (Scheme 2).

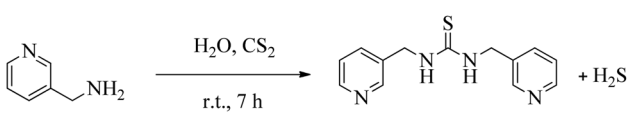

Scheme 1 Synthesis of $(PYT)_2$ ligand (3).

2.4 General procedure for the synthesis of tetrazoles catalyzed by Co-$(PYT)_2$@BNPs

[3 + 2] cycloaddition of NaN_3 with organic nitrile derivatives was used for the formation of tetrazoles in the attendance of Co-$(PYT)_2$@BNPs as nanocatalyst. In this regard, NaN_3 (1.4 mmol) and nitrile (1 mmol) stirred in the attendance of Co-$(PYT)_2$@BNPs (50 mg) in PEG-400 (2 mL) at 120 °C. In the end of the reaction (which checked by TLC), the mixture cooled and was dilute by H_2O and ethyl acetate. Co-$(PYT)_2$@BNPs nanocatalyst isolated *via* simple filtration. Then, HCl (10 mL, 4 N) added and tetrazoles extracted in ethyl acetate. The ethyl acetate solvent dried by anhydrous sodium sulfate and then evaporated (Scheme 3).

2.5 Spectral data

2.5.1 5-Phenyl-1*H*-tetrazole. ^1H NMR (400 MHz, DMSO-d_6): $\delta_H = 16.89$ (br, 1H), 8.06–8.03 (d of d, $J = 8$ Hz, $J = 4$ Hz, 2H), 7.63–7.58 (m, 3H) ppm.

2.5.2 5-(3-nitrophenyl)-1*H*-tetrazole. ^1H NMR (400 MHz, DMSO-d_6): $\delta_H = 17.39$ (br, 1H), 8.85–84 (t, $J = 4$ Hz, 1H), 8.50–8.47 (d of t, $J = 12$ Hz, $J = 4$ Hz, 1H), 8.45–8.41 (d of q, J(d) = 8 Hz, J(q) = 4 Hz, 1H), 7.94–7.89 (t, $J = 12$ Hz, 1H) ppm. ^{13}C NMR (400 MHz, DMSO-d_6): δ_H = 153.9, 147.1, 131.9, 130.0, 125.2, 124.3, 120.3 ppm. IR (KBr) cm^{-1}: 3439, 3092, 2923, 2856, 2700, 1734, 1620, 1527, 1464, 1374, 1161, 1070, 991, 864, 816, 728, 665, 449.

2.5.3 2-(1*H*-tetrazol-5-yl)phenol. ^1H NMR (400 MHz, DMSO-d_6): $\delta_H = 7.99–7.96$ (d of d, $J = 12$ Hz, $J = 4$ Hz, 1H), 7.42–7.37 (t of d, $J = 12$ Hz, 1H), 7.07–7.04 (d, $J = 12$ Hz, 1H), 7.02–6.96 (t, J = 12 Hz, 1H) ppm. ^{13}C NMR (400 MHz, DMSO-d_6): δ_C = 155.3, 151.8, 132.5, 128.9, 119.7, 116.3, 110.6 ppm. IR (KBr) cm^{-1}:3253, 3058, 2941, 2708, 2565, 1892, 1735, 1610, 1546, 1476, 1393, 1358, 1294, 1230, 1150, 1114, 1067, 808, 742, 681, 538, 465.

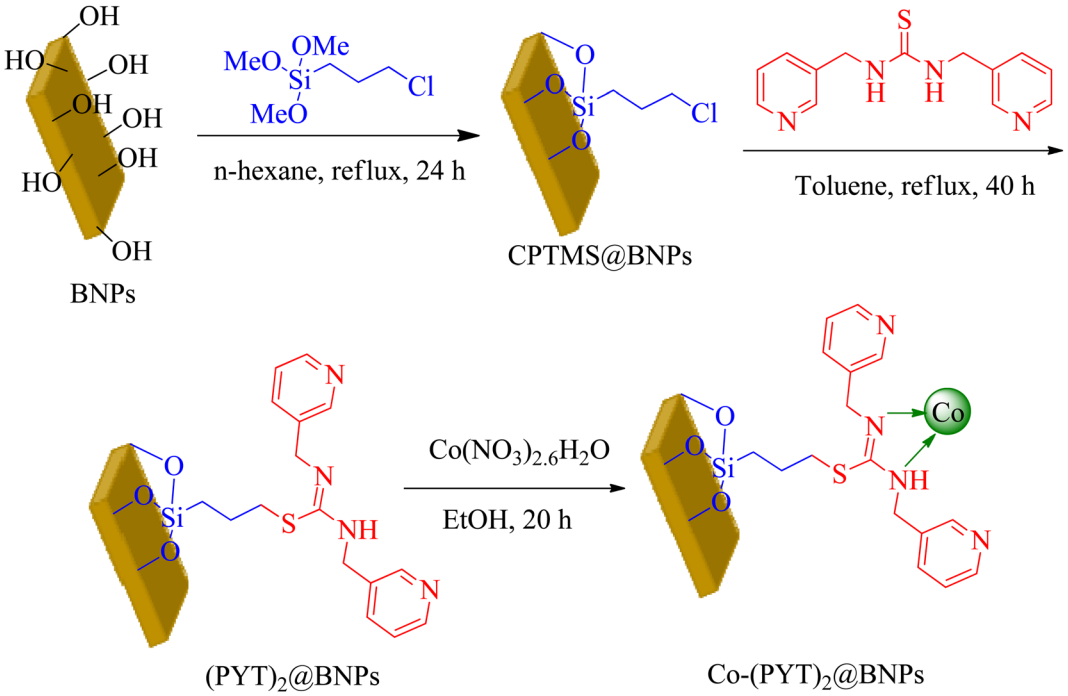

Scheme 2 Synthesis of Co-$(PYT)_2$@BNPs.

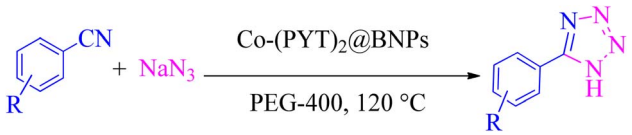

Scheme 3 Synthesis of tetrazoles in the attendance of Co-$(PYT)_2$@BNPs.

3 Results and discussion

3.1 Characterization of the catalyst

At first step, functionalized BNPs by (3-chloropropyl)trimethoxysilane (CPTMS) was produced based on new reported strategy.[41,42] Subsequently, a new complex of cobalt was fabricated on the surface of functionalized BNPs (Co-$(PYT)_2$@BNPs). The catalytic activity of Co-$(PYT)_2$@BNPs was confirmed in the synthesis of tetrazoles. This nanocatalyst was characterized

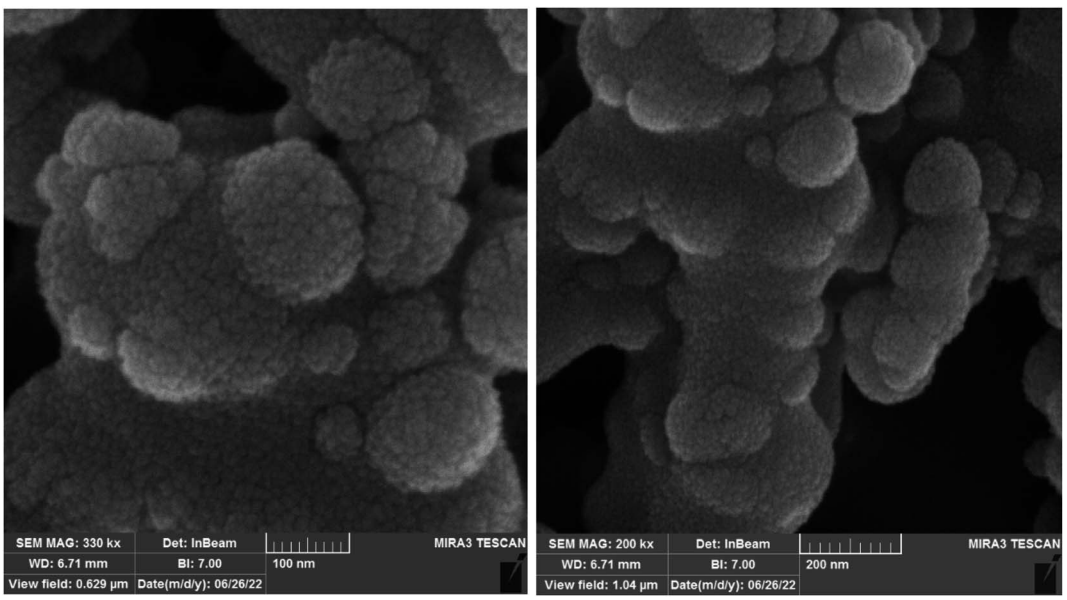

Fig. 1 SEM images of Co-$(PYT)_2$@BNPs.

using Scanning Electron Microscope (SEM), X-ray diffraction (XRD), Fourier transform infrared spectroscopy (FT-IR), wavelength dispersive X-ray spectroscopy (WDX), energy dispersive X-ray spectroscopy (EDS), and thermogravimetric analysis (TGA) techniques.

The shape, morphology, and diameters size of Co-$(PYT)_2$@BNPs studied by FESEM-TESCAN MIRA III Scanning Electron Microscope (SEM) devoice. The SEM images of Co-$(PYT)_2$@BNPs illustrated in Fig. 1. As indicate, the particles of Co-$(PYT)_2$@BNPs formed in uniform spherical shapes and quite homogeneous diameter less than 70 nm.

The obtained results from energy-dispersive X-ray spectroscopy (EDS) analysis of Co-$(PYT)_2$@BNPs are summarized in Fig. 2. As shown, Co-$(PYT)_2$@BNPs is organize from aluminum, oxygen, silicon, nitrogen, carbon, sulfur and cobalt elements. As accepted, the intensity peaks of Al and O elements is sharped than other elements which are formed skeleton of BNPs. Also, the presence of Si, C, N, S and Co elements indicate the successful stabilization of the cobalt complex on BNPs. Also, wavelength dispersive X-ray spectroscopy (WDX) analysis (Fig. 3) illustrate homogeneous distribution of aluminum, oxygen, silicon, nitrogen, carbon,

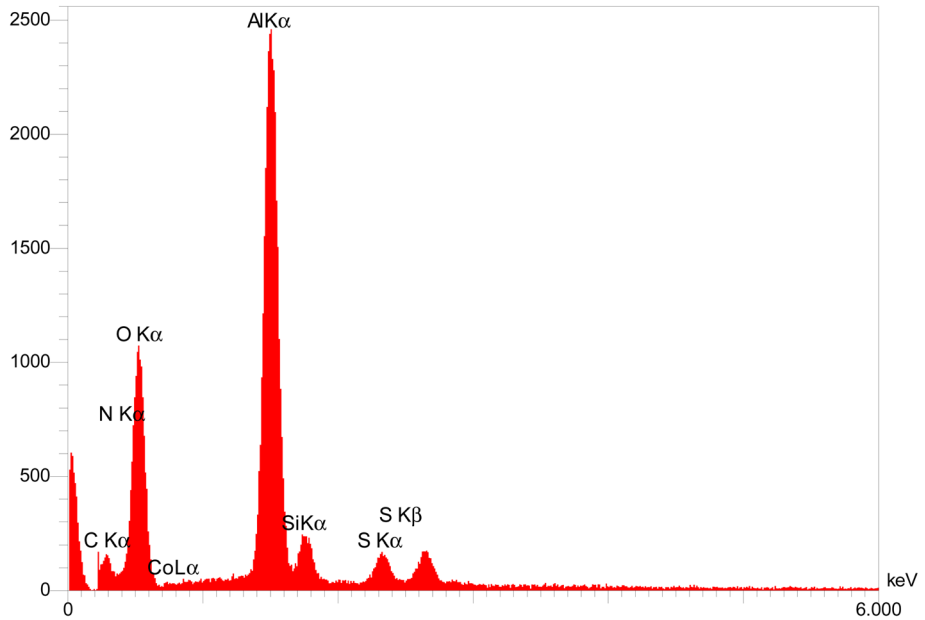

Fig. 2 EDS diagram of Co-$(PYT)_2$@BNPs.

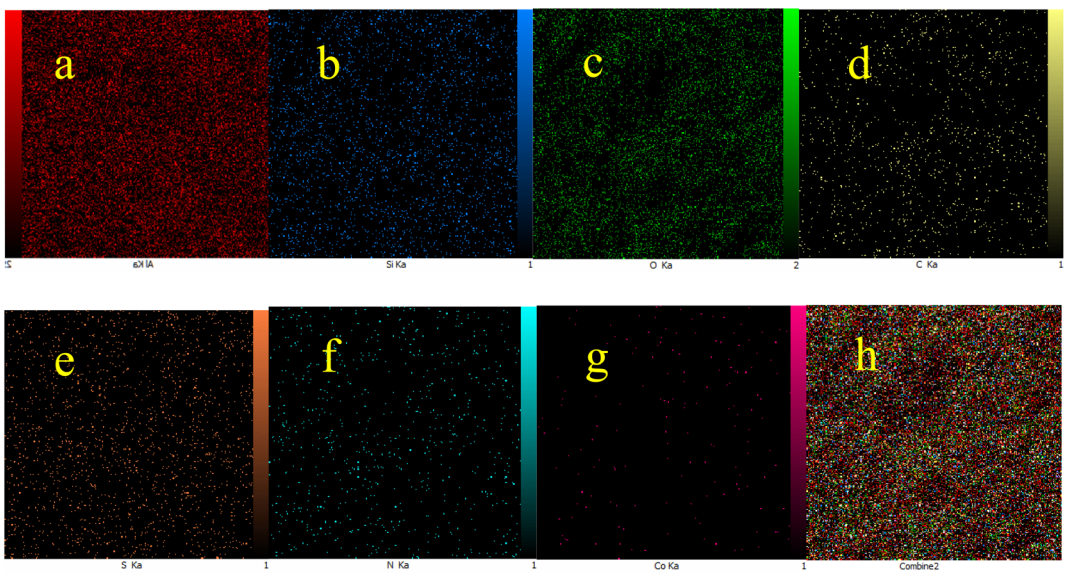

Fig. 3 Elemental mapping of (a) aluminum, (b) silicon, (c) oxygen, (d) carbon, (e) sulfur, (f) nitrogen, (g) cobalt and (h) combine of all elements for Co-$(PYT)_2$@BNPs.

sulfur and cobalt elements in the structure of Co-(PYT)$_2$@BNPs.

TGA analysis can used to determine amount of organic and inorganic content in an organic–inorganic composite samples and also can employed to calculate the thermal stability of materials. Therefore, TGA analysis of Co-(PYT)$_2$@BNPs was performed from 25 °C to 800 °C within increasing temperature rate of 10 °C min^{-1} under air atmosphere (Fig. 4). In TGA diagram of Co-(PYT)$_2$@BNPs, a small weight losses (8% of weight) up to 150 °C is corresponded to the evaporation of solvents.[43] As shown, any weight loss was not indicate up to 250 °C except evaporation of solvents which showed excellent thermal stability of Co-(PYT)$_2$@BNPs. Therefore Co-(PYT)$_2$@-BNPs can be used as catalyst under hard conditions in wide range of organic reactions. TGA analysis of Co-(PYT)$_2$@BNPs illustrated a considerable mass loss (35% of weight) between 250–650 °C which due to the decomposition of immobilized organic layers on the surface of modified BNPs.[44]

X-ray diffraction (XRD) pattern of Co-(PYT)$_2$@BNPs is obtained with Cu Kα radiation (λ = 0.154 nm). As shown in Fig. 5, the XRD pattern of Co-(PYT)$_2$@BNPs shows several peaks of 2θ = 14.69 (0 2 0), 27.89 (1 2 0), 40.34° (0 3 1), 46.84° (1 3 1), 49.89° (0 5 1), 53.99° (2 0 0), 56.54° (1 5 1), 58.59° (0 8 0), 63.74° (2 3 1), 65.64° (0 0 2), 67.74° (1 7 1), and 72.89° (2 5 1) that confirm BNPs is stable in orthorhombic unit cell[2,4] after stabilization of cobalt complex. The intensity of all peaks was decreased than BNPs due to the chemical modifications of BNPs.[33] Also, a broad peak of 2θ from 15° to 25° related to the amorphous SiO_2.[45] Also, XRD pattern of Co-(PYT)$_2$@BNPs showed four peaks at 2θ = 15.79° (1 1 0), 32.44°

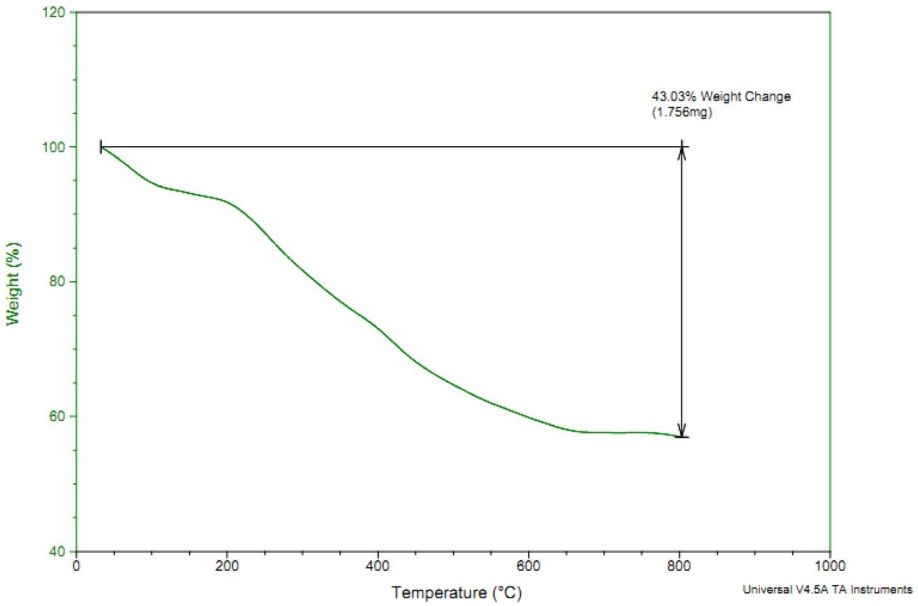

Fig. 4 TGA diagram of Co-(PYT)$_2$@BNPs.

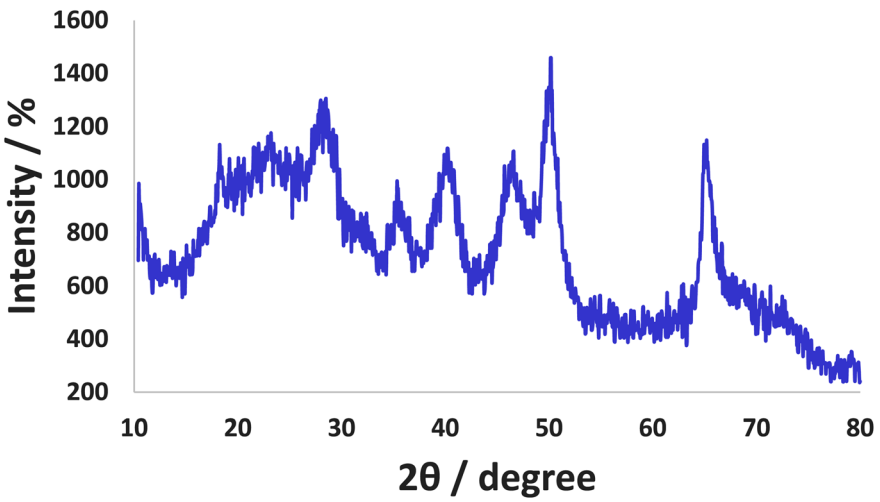

Fig. 5 Normal XRD pattern of Co-(PYT)$_2$@BNPs.

(2 2 0), 54.19° (1 4 1) and 63.14° (5 0 3) which can be related to Cobalt(II) species.[33]

The FT-IR spectrum of CPTMS@BNPs, (b) $(PYT)_2$@BNPs, and (c) Co-$(PYT)_2$@BNPs shown in Fig. 6. Bands vibration at low wavenumbers <750 cm^{-1} in the FT-IR spectra related to the vibrations of the Al–O bonds.[4] O–H and N–H bands appeared above 3000 cm^{-1} in the FT-IR spectra.[46] In addition, the stretching vibrations of Si–O identified in region 805 cm^{-1} and 1075 cm^{-1} of FT-IR spectra.[41,47] In addition, stretching vibrations of the C=N groups have appeared in the 1635 cm^{-1} region.[4,48]

3.2 Catalytic studying of the catalyst

After characterization of Co-$(PYT)_2$@BNPs, it was used as efficient, recyclable and biocompatible nanocatalyst in the synthesis of tetrazole heterocyclic compounds. The best reaction conditions obtained through [3 + 2] cycloaddition of NaN_3 and benzonitrile as model reaction (Table 1). The model reaction did not taken place in the absence of Co-$(PYT)_2$@BNPs nanocatalyst (Table 1, entry 1). While, the presentence of Co-$(PYT)_2$@BNPs is required for the synthesis of 5-substituted 1*H*-tetrazole heterocyclic compounds. As expected, the model reaction occurs with the addition of catalyst and it faster proceeded by increasing in amount of Co-$(PYT)_2$@BNPs catalyst. As shown, the model reaction completed within acceptable time when the amount of catalyst increased up to 50 mg (Table 1, entry 3). Among of several solvents (such as H_2O, DMSO and PEG-400) which are examined, PEG-400 was provided the best results in term of reaction time and isolated yield of the pure product (Table 1, entry 3). Also, the effect of equivalent amount of NaN_3 to benzonitrile and temperature on the model reaction was studied, which the best results were obtained with 1.4 mmol of NaN_3 per 1 mmol of benzonitrile at 120 °C (Table 1, entry 3).

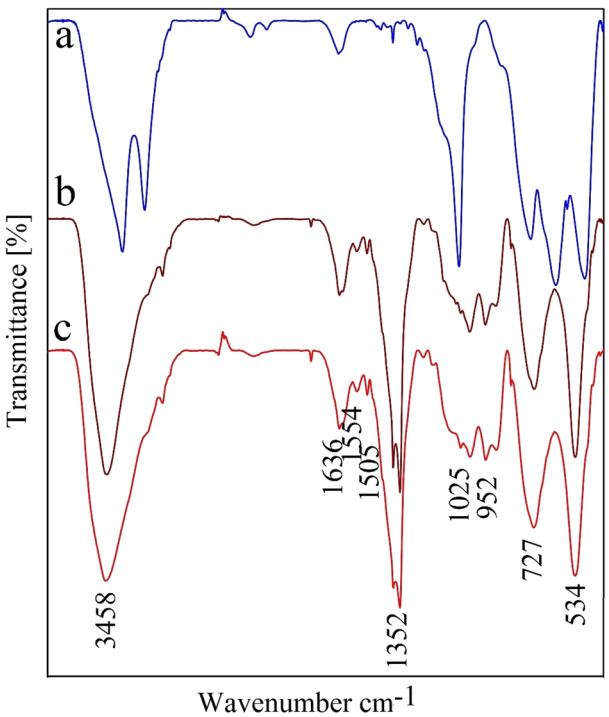

Fig. 6 FT-IR spectra of (a) CPTMS@BNPs, (b) $(PYT)_2$@BNPs, and (c) Co-$(PYT)_2$@BNPs.

The scope of catalytic application of Co-$(PYT)_2$@BNPs nanocatalyst was extended in the [3 + 2] cycloaddition of NaN_3 and other benzonitrile derivatives (Table 2). In this regard, several benzonitrile compounds with an electron-withdrawing or electron-donating groups on *para*- *meta*- or *ortho*-position of aromatic ring were examined under optimized reaction conditions in hand. As shown in Table 2, all corresponding heterocyclic tetrazoles were produced in good yields. Also, phthalonitrile was employed as nitrile substrate which has two similar cyano groups on 1,2 position of its aromatic ring (Table 2, entry 4). As shown in Table 2 (entry 4), this methodology was provided only monoaddition which may be related to steric hindrance or selectivity of this catalyst. Also [1,1′-biphenyl]-4-carbonitrile (4-phenyl benzonitrile) was synthesized based on recently reported literature[49] and it was investigated in the [3 + 2] cycloaddition reaction with NaN_3 (Table 2, entry 11).

Based on reported authentic methodologies about synthesis of tetrazoles in the presence of immobilized transition metal catalysts,[46,54] a mechanism cycle for the synthesis of tetrazoles in the presence of Co-$(PYT)_2$@BNPs catalyst offered in Scheme 4.

3.3 Reusability of the catalyst

As mentioned, Co-$(PYT)_2$@BNPs catalyst is stable and it has heterogeneity nature. Therefore the reusability and

Table 1 Optimizing the best conditions for the synthesis of tetrazoles in the presence of Co-$(PYT)_2$@BNPs nanocatalyst

Entry	Amount of the catalyst (mg)	Solvent	NaN_3 (mmol)	Time (min)	Temperature (°C)	Yield (%)[a]
1	—	PEG	1.4	150	120	N. R.[b]
2	40	PEG	1.4	310	120	85
3	50	PEG	1.4	100	120	98
4	50	PEG	1.3	120	120	80
5	50	DMSO	1.4	100	120	81
6	50	H_2O	1.4	100	Reflux	20
7	50	PEG	1.4	100	100	49

[a] Isolated yield within 120 min. [b] No reaction.

Table 2 Synthesis of 5-substituted 1*H*-tetrazole derivatives catalyzed by Co-$(PYT)_2$@BNPs nanocatalyst

Entry	Nitrile	Product	Time (min)	Yield (%)[a]	Melting point	Reference
1	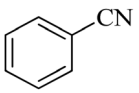	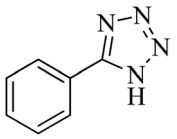	120	98	214–215	36
2	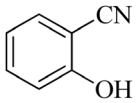	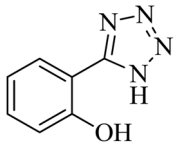	180	94	223–226	41
3	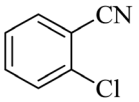	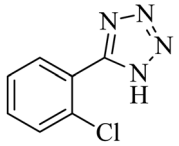	200	95	179–181	36
4	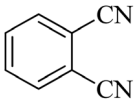	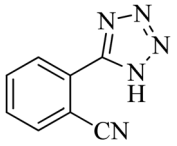	50	93	210–211	41
5	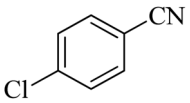	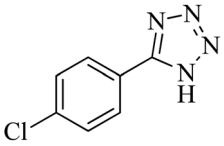	190	96	261–262	36
6	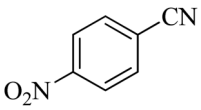	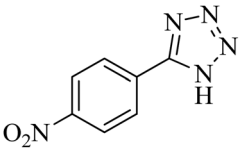	405	98	217–220	40
7	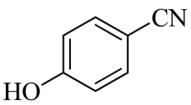	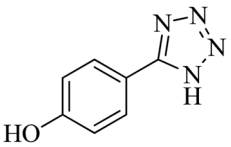	50	93	229–231	40
9	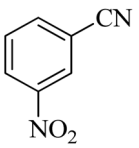	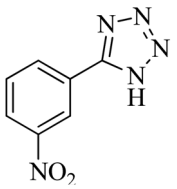	360	95	149–151	44
10	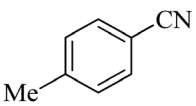	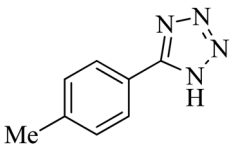	16 h	89	247–249	50 and 51
11	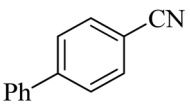	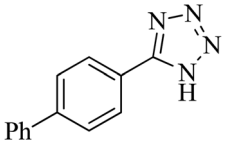	46 h	71	245–248	52 and 53

[a] Isolated yield.

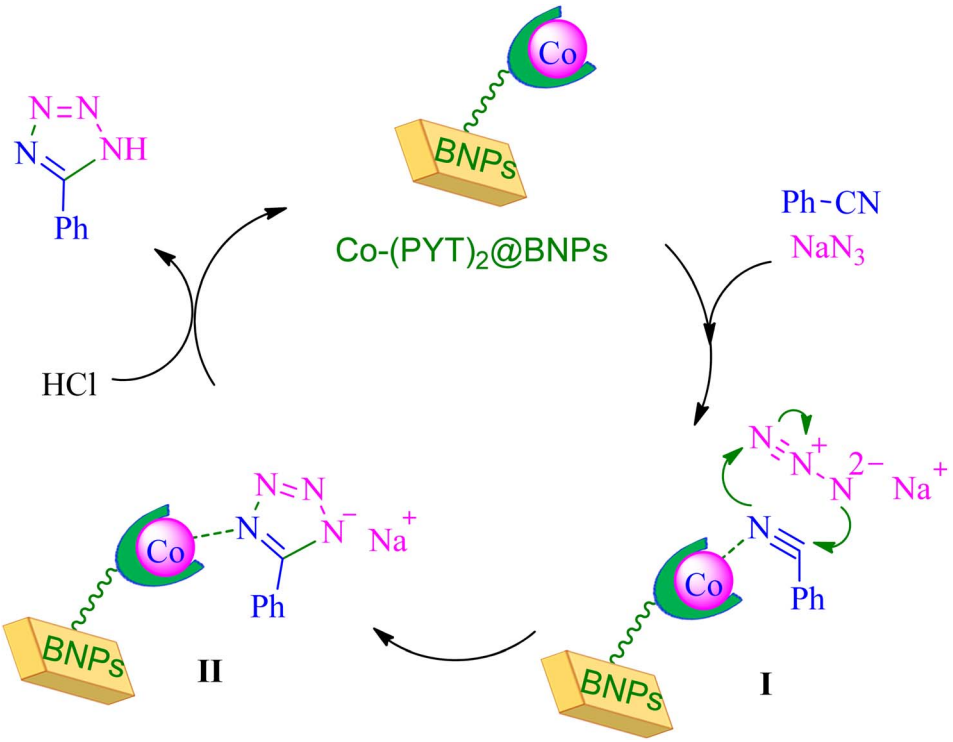

Scheme 4 Expected mechanism for the synthesis of tetrazoles in the presence of Co-$(PYT)_2$@BNPs nanocatalyst.

retrievability of Co-$(PYT)_2$@BNPs nanocatalyst were investigated in the [3 + 2] cycloaddition of benzonitrile and NaN_3 for the synthesis of 5-phenyl-1*H*-tetrazole. As shown in Fig. 7, Co-$(PYT)_2$@BNPs catalyst can be recovered and reused up to 6 runs without any further activation.

3.4 Comparison of the catalyst

The efficiency and advantages of Co-$(PYT)_2$@BNPs catalyst than previous reported catalysts were compared in the [3 + 2] cycloaddition of benzonitrile with sodium azide in the presence of Co-$(PYT)_2$@BNPs and previous catalysts (Table 3). As shown, Co-$(PYT)_2$@BNPs catalyst afford 98% of 5-phenyl-1*H*-tetrazole product in 2 h which is better than previous reported catalysts in terms of time and yields. Also, some of previous catalysts have several disadvantages, limitations or drawbacks such as low yield of the products, long reaction times, expensive catalysts, non-environmental conditions, non or difficult separation of the catalysts and utilize hazard solvents. While, in this work, the synthesis of tetrazoles was introduced in the presence of Co-$(PYT)_2$@BNPs as reusable catalyst in green solvent such as PEG, in short reaction time with acceptable yield.

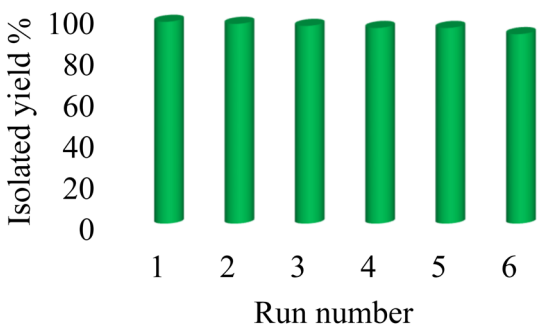

Fig. 7 The reusability of Co-$(PYT)_2$@BNPs in the synthesis of 5-phenyl-1*H*-tetrazole.

Table 3 Comparison results of Co-$(PYT)_2$@BNPs nanocatalyst with other catalysts for synthesis of 5-phenyl-1*H*-tetrazole

Entry	Catalyst	Time (h)	Yield (%)	Ref.
1	CoY zeolite	14	90	37
2	Cu–Zn alloy nanopowder	10	95	55
3	$B(C_6F_5)_3$	8	94	56
4	Fe_3O_4@SiO_2/Salen Cu(II)	7	90	57
5	Fe_3O_4/ZnS HNSs	24	81.1	58
6	Pd-isatin-boehmite	8	94	59
7	Mesoporous ZnS	36	86	60
8	$AgNO_3$	5	83	61
9	$CuFe_2O_4$	12	82	62
10	Nano ZnO/Co_3O_4	12	90	63
11	Pd-SMTU@boehmite	2.5	95	64
12	Cu-TBA@biochar	7	98	41
13	L-cysteine-Pd@MCM-41	3	98	65
14	Ni-MP(AMP)$_2$@Fe-biochar	3.8	92	34
15	Cu(II)-adenine-MCM-41	5	92	66
16	Pd-Arg@boehmite	7	97	36
17	Cu-DABP@Fe_3O_4/MCM-41	2	99	46
18	Fe_3O_4@boehmite NPs	4	97	67
19	Co-$(PYT)_2$@BNPs	2	98	This work

4 Conclusions

In Conclusion, we synthesized a new stabilized complex of cobalt on modified boehmite NPs by 1,3-bis(pyridin-3-ylmethyl) thiourea (Co-$(PYT)_2$@BNPs) as highly practical, retrievable, stable, and maintainable organic–inorganic hybrid nanocatalyst. Co-$(PYT)_2$@BNPs was characterized by various techniques such as XRD, TGA, SEM, EDS, WDX and FT-IR. Catalytic activity of this catalyst was studied in the formation of organic heterocyclic compounds such as tetrazole derivatives. Co-$(PYT)_2$@BNPs display high activity, stability and recyclability in the synthesis of tetrazoles.

Conflicts of interest

There are no conflicts to declare.

Acknowledgements

Pecuniary support for this work by the research affairs of Islamic Azad University, Qeshm Branch, Qeshm, Iran is gratefully acknowledged. Also, authors appreciate Ilam University for pecuniary support of this research project.

References

1 J. Karger-Kocsis and L. Lendvai, Polymer/boehmite nanocomposites: A review, *J. Appl. Polym. Sci.*, 2018, **135**, 45573.
2 M. Mohammadi, M. Khodamorady, B. Tahmasbi, K. Bahrami and A. Ghorbani-Choghamarani, Boehmite nanoparticles as versatile support for organic–inorganic hybrid materials: Synthesis, functionalization, and applications in eco-friendly catalysis, *J. Ind. Eng. Chem.*, 2021, **97**, 1.
3 Y. Xie, D. Kocaefe, Y. Kocaefe, J. Cheng and W. Liu, The Effect of Novel Synthetic Methods and parameters Control on Morphology of nano-alumina Particles, *Nanoscale Res. Lett.*, 2016, **11**, 259.
4 A. Jabbari, P. Moradi, M. Hajjami and B. Tahmasbi, Tetradentate copper complex supported on boehmite nanoparticles as an efficient and heterogeneous reusable nanocatalyst for the synthesis of diaryl ethers, *Sci. Rep.*, 2022, **12**, 11660.
5 L. Rajabi and A. A. Derakhshan, Room Temperature Synthesis of Boehmite and Crystallization of Nanoparticles: Effect of Concentration and Ultrasound, *Sci. Adv. Mater.*, 2010, **2**, 163.
6 M. F. Peintinger, M. J. Kratz and T. Bredow, Quantum-chemical study of stable, meta-stable and high-pressure alumina polymorphs and aluminum hydroxides, *J. Mater. Chem. A*, 2014, **2**, 13143.
7 S. Bruhne, S. Gottlieb, W. Assmus, E. Alig and M. U. Schmidt, Atomic structure analysis of nanocrystalline boehmite AlO(OH), *Cryst. Growth Des.*, 2008, **8**, 489.
8 J. Karger-Kocsis and L. Lendvai, Polymer/boehmite nanocomposites: A review, *J. Appl. Polym. Sci.*, 2018, **135**, 45573.
9 A. Ghorbani-Choghamarani, M. Hajjami, B. Tahmasbi and N. Noori, Boehmite silica sulfuric acid: as a new acidic material and reusable heterogeneous nanocatalyst for the various organic oxidation reactions, *J. Iran. Chem. Soc.*, 2016, **13**, 2193–2202.
10 J. Fankhanel, D. Silbernagl, M. Ghasem Zadeh Khorasani, B. Daum, A. Kempe, H. Sturm and R. Rolfes, Mechanical Properties of Boehmite Evaluated by Atomic Force Microscopy Experiments and Molecular Dynamic Finite Element Simulations, *J. Nanomater.*, 2016, **2016**, 13.
11 A. Ghorbani-Choghamarani, Z. Heidarnezhad and B. Tahmasbi, New Complex of Copper on Boehmite Nanoparticles as Highly Efficient and Reusable Nanocatalyst for Synthesis of Sulfides and Ethers, *ChemistrySelect*, 2019, **4**, 1.
12 M. Faisal, Z. U. Rehman, Q. Aein and A. Saeed, Terpyridine-Pr-Fe_3O_4@boehmite nanoparticles; a novel and highly effective magnetic nanocatalyst for preparation of cyclic carbonates from carbon dioxide and epoxides under solventless conditions, *Mater. Chem. Phys.*, 2019, **231**, 272.
13 R. P. C. Rajan, V. Sekar and V. Sivan, Boehmite an Efficient and Recyclable Acid–Base Bifunctional Catalyst for Aldol Condensation Reaction, *J. Nanosci. Nanotechnol.*, 2018, **18**, 4270.
14 A. Ghorbani-Choghamarani, P. Moradi and B. Tahmasbi, Modification of boehmite nanoparticles with Adenine for the immobilization of Cu(II) as organic–inorganic hybrid nanocatalyst in organic reactions, *Polyhedron*, 2019, **163**, 98.
15 D. Mishra, S. Anand, R. K. Panda and R. P. Das, Hydrothermal preparation and characterization of boehmites, *Mater. Lett.*, 2000, **42**, 38.
16 L. Candela and D. D. Perlmutter, Kinetics of boehmite formation by thermal decomposition of gibbsite, *Ind. Eng. Chem. Res.*, 1992, **31**, 694.
17 M. Nguefack, A. F. Popa, S. Rossignol and C. Kappenstein, Preparation of alumina through a sol–gel process. Synthesis, characterization, thermal evolution and model of intermediate boehmite, *Phys. Chem. Chem. Phys.*, 2003, **5**, 4279.
18 D. G. Lewis and V. C. Farmer, Infrared absorption of surface hydroxyl groups and lattice vibrations in lepidocrocite (γ-FeOOH) and boehmite (γ-AlOOH), *Clay Miner.*, 1986, **21**, 93.
19 Y. Jia, B. S. Zhu, Z. Jin, B. Sun, T. Luo, X. Y. Yu, L. T. Kong and J. H. Liu, Fluoride removal mechanism of bayerite/boehmite nanocomposites: Roles of the surface hydroxyl groups and the nitrate anions, *J. Colloid Interface Sci.*, 2015, **440**, 60.
20 P. Raybaud, M. Digne, R. Iftimie, W. Wellens, P. Euzen and H. Toulhoat, Morphology and Surface Properties of Boehmite (γ-AlOOH): A Density Functional Theory Study, *J. Catal.*, 2001, **201**, 236.
21 S. A. Dickie and A. J. McQuillan, In Situ Infrared Spectroscopic Studies of Adsorption Processes on Boehmite Particle Films: Exchange of Surface Hydroxyl

Groups Observed upon Chelation by Acetylacetone, *Langmuir*, 2004, **20**, 11630.

22 A. Ghorbani-Choghamarani, Z. Seydyosefi and B. Tahmasbi, Tribromide ion supported on boehmite nanoparticles as a reusable catalyst for organic reactions, *C. R. Chim.*, 2018, **21**, 1011.

23 R. Doosti, M. Bakherad, M. Mirzaee and K. Jadidi, Boehmite Silylpropyl Amine Sulfamic Acid as an Efficient and Recyclable Catalyst for the Synthesis of some Pyrazole Derivatives, *Lett. Org. Chem.*, 2017, **14**, 450.

24 A. Ghorbani-Choghamarani, Z. Heidarnezhad, B. Tahmasbi and G. Azadi, TEDETA@BNPs as a basic and metal free nanocatalyst for Knoevenagel condensation and Hantzsch reaction, *J. Iran. Chem. Soc.*, 2018, **15**, 2281.

25 M. Mirzaee, B. Bahramian, P. Gholampour, S. Teymouri and T. Khorsand, Preparation and characterization of Fe_3O_4@Boehmite core–shell nanoparticles to support molybdenum or vanadium complexes for catalytic epoxidation of alkenes, *Appl. Organomet. Chem.*, 2019, **33**, e4792.

26 S. Roy, K. Pal, S. Bardhan, S. Maity, D. K. Chanda, S. Ghosh, P. Karmakar and S. Das, Gd(III)-Doped Boehmite Nanoparticle: An Emergent Material for the Fluorescent Sensing of Cr(VI) in Wastewater and Live Cells, *Inorg. Chem.*, 2019, **58**, 8369.

27 A. P. Panda, U. Jha and S. K. Swain, Synthesis of nanostructured copper oxide loaded boehmite (CuO_Boehmite) for adsorptive removal of As(III/V) from aqueous solution, *J. Water Process. Eng.*, 2020, **37**, 101506.

28 V. Claude, J. G. Mahy, T. Lohay, J. Geens and S. D. Lambert, Coating Process of Honeycomb Cordierite Support with Ni/Boehmite Gels, *Processes*, 2022, **10**, 875.

29 X. Li, Influence of melamine cyanurate and boehmite on flame retardancy of PA6, *Iran. Polym. J.*, 2022, **31**, 975.

30 C. B. Nettar, R. N. Bhowmik and A. K. Sinha, A comparative study of the lattice structure, optical band gap, electrical conductivity and polarization at different stages of the heat treatment of chemical routed $Al(OH)_3$, *Ceram. Int.*, 2022, **48**, 10677.

31 H. Wang, S. T. B. Lundin, K. Takanabe and S. T. Oyama, Synthesis of size-controlled boehmite sols: application in high-performance hydrogen-selective ceramic membranes, *Mater. Chem. A*, 2022, **10**, 12869.

32 Z. Liang, X. Wang, G. Yu, M. Li, S. Shi, H. Bao, C. Chen, D. Fu, W. Ma, C. Xue and B. Sun, Mechanistic understanding of the aspect ratio-dependent adjuvanticity of engineered aluminum oxyhydroxide nanorods in prophylactic vaccines, *Nano Today*, 2022, **43**, 101445.

33 A. Mohammadinezhad and B. Akhlaghinia, Fe_3O_4@Boehmite-NH_2-CoII NPs: an inexpensive and highly efficient heterogeneous magnetic nanocatalyst for the Suzuki–Miyaura and Heck–Mizoroki cross-coupling reactions, *Green Chem.*, 2017, **19**, 5625.

34 P. Moradi and M. Hajjami, Magnetization of biochar nanoparticles as a novel support for fabrication of organo nickel as a selective, reusable and magnetic nanocatalyst in organic reactions, *New J. Chem.*, 2021, **45**, 2981.

35 M. A. K. Zarchi and F. Nazem, Using a polymer-supported azide ion in [2 + 3] cycloaddition reaction of azide ion with nitriles, *J. Appl. Polym. Sci.*, 2012, **123**, 1977.

36 B. Tahmasbi and A. Ghorbani-Choghamarani, First report of the direct supporting of palladium–arginine complex on boehmite nanoparticles and application in the synthesis of 5-substituted tetrazoles, *Appl. Organomet. Chem.*, 2017, **31**, e3644.

37 V. Rama, K. Kanagaraj and K. Pitchumani, Syntheses of 5-Substituted 1*H*-Tetrazoles Catalyzed by Reusable CoY Zeolite, *J. Org. Chem.*, 2011, **76**, 9090.

38 S. S. E. Ghodsinia and B. Akhlaghinia, A rapid metal free synthesis of 5-substituted-1*H*-tetrazoles using cuttlebone as a natural high effective and low cost heterogeneous catalyst, *RSC Adv.*, 2015, **5**, 49849.

39 Z. P. Demko and K. B. Sharpless, Preparation of 5-Substituted 1*H*-Tetrazoles from Nitriles in Water, *J. Org. Chem.*, 2001, **66**, 7945.

40 M. Nikoorazm, B. Tahmasbi, S. Gholami and P. Moradi, Copper and nickel immobilized on cytosine@MCM-41: as highly efficient, reusable and organic–inorganic hybrid nanocatalysts for the homoselective synthesis of tetrazoles and pyranopyrazoles, *Appl. Organomet. Chem.*, 2020, **34**, e5919.

41 P. Moradi, M. Hajjami and B. Tahmasbi, Fabricated copper catalyst on biochar nanoparticles for the synthesis of tetrazoles as antimicrobial agents, *Polyhedron*, 2020, **175**, 114169.

42 B. Tahmasbi, M. Nikoorazm, P. Moradi and Y. Abbasi Tyula, A Schiff base complex of lanthanum on modified MCM-41 as a reusable nanocatalyst in the homoselective synthesis of 5-substituted 1*H*-tetrazoles, *RSC Adv.*, 2022, **12**, 34303–34317.

43 A. Rezaei, A. Ghorbani-Choghamarani and B. Tahmasbi, Synthesis and Characterization of Nickel Metal-Organic Framework Including 4,6-diamino-2-mercaptopyrimidine and its Catalytic Application in Organic Reactions, *Catal. Lett.*, 2022, DOI: **10.1007/s10562-022-04135-8**.

44 M. Nikoorazm, Z. Rezaei and B. Tahmasbi, Two Schiff-base complexes of copper and zirconium oxide supported on mesoporous MCM-41 as an organic–inorganic hybrid catalysts in the chemo and homoselective oxidation of sulfides and synthesis of tetrazoles, *J. Porous Mater.*, 2020, **27**, 671.

45 B. Tahmasbi, A. Ghorbani-Choghamarani and P. Moradi, Palladium fabricated on boehmite as an organic–inorganic hybrid nanocatalyst for C–C cross coupling and homoselective cycloaddition reactions, *New J. Chem.*, 2020, **44**, 3717.

46 T. Kikhavani, P. Moradi, M. Mashari-Karir and J. Naji, A new copper Schiff-base complex of 3,4-diaminobenzophenone stabilized on magnetic MCM-41 as a homoselective and reusable catalyst in the synthesis of tetrazoles and pyranopyrazoles, *Appl. Organomet. Chem.*, 2022, **36**, e6895.

47 P. Moradi and M. Hajjami, Magnetization of graphene oxide nanosheets using nickel magnetic nanoparticles as a novel support for the fabrication of copper as a practical,

selective, and reusable nanocatalyst in C–C and C–O coupling reactions, *RSC Adv.*, 2021, **11**, 25867.

48 M. Nikoorazm, P. Moradi, N. Noori and G. Azadi, L-Arginine complex of copper on modified core–shell magnetic nanoparticles as reusable and organic–inorganic hybrid nanocatalyst for the chemoselective oxidation of organosulfur compounds, *J. Iran. Chem. Soc.*, 2021, **18**, 467.

49 P. Moradi and M. Hajjami, Stabilization of ruthenium on biochar-nickel magnetic nanoparticles as a heterogeneous, practical, selective, and reusable nanocatalyst for the Suzuki C–C coupling reaction in water, *RSC Adv.*, 2022, **12**, 13523–13534.

50 E. Aali, M. Gholizadeh and N. Noroozi-Shad, 1-Disulfo-[2,2-bipyridine]-1,1-diium chloride ionic liquid as an efficient catalyst for the green synthesis of 5-substituted 1H-tetrazoles, *J. Mol. Struct.*, 2022, **1247**, 131289.

51 M. Aqeel Ashraf, Z. Liu, C. Li and D. Zhang, Fe_3O_4@L-lysine-Pd(0) organic–inorganic hybrid: As a novel heterogeneous magnetic nanocatalyst for chemo and homoselective [2 + 3] cycloaddition synthesis of 5-substituted 1*H*-tetrazoles, *Appl. Organomet. Chem.*, 2020, **35**, e6133.

52 K. Uchida and H. Togo, Transformation of aromatic bromides into aromatic nitriles with *n*-BuLi, pivalonitrile, and iodine under metal cyanide-free conditions, *Tetrahedron*, 2019, **75**, 130550.

53 B. Sreedhar, A. Suresh Kumar and D. Yada, CuFe2O4 nanoparticles: a magnetically recoverable and reusable catalyst for the synthesis of 5-substituted 1*H*-tetrazoles, *Tetrahedron Lett.*, 2011, **52**, 3565–3569.

54 P. Moradi, B. Zarei, Y. Abbasi Tyulaa and M. Nikoorazm, Novel neodymium complex on MCM-41 magnetic nanocomposite as a practical, selective and returnable nanocatalyst in the synthesis of tetrazoles with antifungal properties in agricultural, *Appl. Organometal. Chem.*, 2023, **37**, e7020.

55 G. Aridoss and K. K. Laali, Highly Efficient Synthesis of 5-Substituted 1*H*-Tetrazoles Catalyzed by Cu–Zn Alloy Nanopowder, Conversion into 1,5- and 2,5-Disubstituted Tetrazoles, and Synthesis and NMR Studies of New Tetrazolium Ionic Liquids, *Eur. J. Org. Chem.*, 2011, 6343.

56 S. Kumar Prajapti, A. Nagarsenkar and B. Nagendra Babu, An efficient synthesis of 5-substituted 1*H*-tetrazoles via $B(C_6F_5)_3$ catalyzed [3 + 2] cycloaddition of nitriles and sodium azide, *Tetrahedron Lett.*, 2014, **55**, 3507.

57 F. Dehghani, A. R. Sardarian and M. Esmaeilpour, Salen complex of Cu(II) supported on superparamagnetic Fe_3O_4@SiO_2 nanoparticles: An efficient and recyclable catalyst for synthesis of 1- and 5-substituted 1*H*-tetrazoles, *J. Organomet. Chem.*, 2013, **743**, 87.

58 G. Qi, W. Liu and Z. Bei, Fe_3O_4/ZnS Hollow Nanospheres: A Highly Efficient Magnetic Heterogeneous Catalyst for Synthesis of 5-Substituted 1*H* -Tetrazoles from Nitriles and Sodium Azide, *Chin. J. Chem.*, 2011, **29**, 131.

59 A. Jabbari, B. Tahmasbi, M. Nikoorazm and A. Ghorbani-Choghamarani, A new Pd-Schiff-base complex on boehmite nanoparticles: Its application in Suzuki reaction and synthesis of tetrazoles, *Appl. Organometal. Chem.*, 2018, **32**, e4295.

60 L. Lang, H. Zhou, M. Xue, X. Wang and Z. Xu, Mesoporous ZnS hollow spheres-catalyzed synthesis of 5-substituted 1*H*-tetrazoles, *Mater. Lett.*, 2013, **106**, 443.

61 P. Mani, A. K. Singh and S. K. Awasthi, $AgNO_3$ catalyzed synthesis of 5-substituted-1*H*-tetrazole via [3 + 2] cycloaddition of nitriles and sodium azide, *Tetrahedron Lett.*, 2014, **55**, 1879.

62 B. Sreedhar, A. Suresh Kumar and D. Yada, $CuFe_2O_4$ nanoparticles: a magnetically recoverable and reusable catalyst for the synthesis of 5-substituted 1*H*-tetrazoles, *Tetrahedron Lett.*, 2011, **52**, 3565.

63 S. M. Agawane and J. M. Nagarkar, Synthesis of 5-substituted 1*H*-tetrazoles using a nano ZnO/Co_3O_4 catalyst, *Catal. Sci. Technol.*, 2012, **2**, 1324.

64 P. Moradi and A. Ghorbani-Choghamarani, Efficient synthesis of 5-substituted tetrazoles catalysed by palladium–S-methylisothiourea complex supported on boehmite nanoparticles, *Appl. Organometal. Chem.*, 2017, **31**, e3602.

65 M. Nikoorazm, P. Moradi and N. Noori, L-cysteine complex of palladium onto mesoporous channels of MCM-41 as reusable, homoselective and organic–inorganic hybrid nanocatalyst for the synthesis of tetrazoles, *J. Porous Mater.*, 2020, **27**, 1159.

66 M. Nikoorazm, A. Ghorbani-Choghamaranai, M. Khanmoradi and P. Moradi, Synthesis and characterization of Cu(II)-Adenine-MCM-41 as stable and efficient mesoporous catalyst for the synthesis of 5-substituted 1*H*-tetrazoles and 1*H*-indazolo [1,2-b] phthalazine-triones, *J. Porous Mater.*, 2018, **25**, 1831.

67 P. Moradi, Investigation of Fe_3O_4@boehmite NPs as efficient and magnetically recoverable nanocatalyst in the homoselective synthesis of tetrazoles, *RSC Adv.*, 2022, **12**, 33459–33468.